CFD AND EXPERIMENTAL INVESTIGATION OF SLOSHING PARAMETERS FOR THE SAFETY ASSESSMENT OF HLM REACTORS

Konstantinos Myrillas, Philippe Planquart and Jean-Marie Buchlin
von Karman Institute for Fluid Dynamics
Chaussée de Waterloo 72, B-1640 Rhode-St-Genèse, Belgium
myrillas@vki.ac.be; philippe.planquart@vki.ac.be; buchlin@vki.ac.be

Marc Schyns
SCK·CEN
Boeretang 200, B-2400 Mol, Belgium
mschyns@SCKCEN.BE

ABSTRACT

For the safety assessment of Heavy Liquid Metal nuclear reactors under seismic excitation, sloshing phenomena can be of great concern. The earthquake motions are transferred to the liquid coolant which oscillates inside the vessel, exerting additional forces on the walls and internal structures. The present study examines the case of MYRRHA, a multi-purpose experimental reactor with LBE as coolant, developed by SCK·CEN. The sloshing behavior of liquid metals is studied through a comparison between mercury and water in a cylindrical tank. Experimental investigation of sloshing is carried out using optical techniques with the shaking table facility SHAKESPEARE at the von Karman Institute. Emphasis is given on the resonance case, where maximum forces occur on the tank walls. The experimental cases are reproduced numerically with the CFD software OpenFOAM, using the VOF method to track the liquid interface. The non-linear nature of sloshing is observed through visualization, where swirling is shown in the resonance case. The complex behavior is well reproduced by the CFD simulations, providing good qualitative validation of the numerical tools. A quantitative comparison of the maximum liquid elevation inside the tank shows higher values for the liquid metal than for water. Some discrepancies are revealed in CFD results and the differences are quantified. From simulations it is verified that the forces scale with the density ratio, following similar evolution in time. Overall, water is demonstrated to be a valid option as a working liquid in order to evaluate the sloshing effects, for forcing frequencies up to resonance.

KEYWORDS
Sloshing, CFD, experiments, HLM, resonance

1. INTRODUCTION

Seismic safety of nuclear reactors is of primary importance and it has been brought to focus even more after the Fukushima I Nuclear Power Plant was struck by the violent (magnitude 9.0) Tōhoku earthquake and tsunami in March 2011. For a partially filled Heavy Liquid Metal (HLM) nuclear reactor under seismic excitation, large liquid motions, known as *sloshing*, can introduce extra loads on the structures and internal components [1]. These loads are hard to predict because of the non-linear nature of sloshing, but prediction methods are necessary for the safety assessment. The present study refers to MYRRHA (Multi-purpose hYbrid Research Reactor for High-tech Applications), which is a versatile experimental Accelerator-Driven System (ADS) under development at the SCK•CEN, the Belgian Nuclear Research

Centre [2]. It is designed to use Lead-Bismuth-Eutectic (LBE) alloy as liquid coolant and a schematic is presented in Fig. 1.
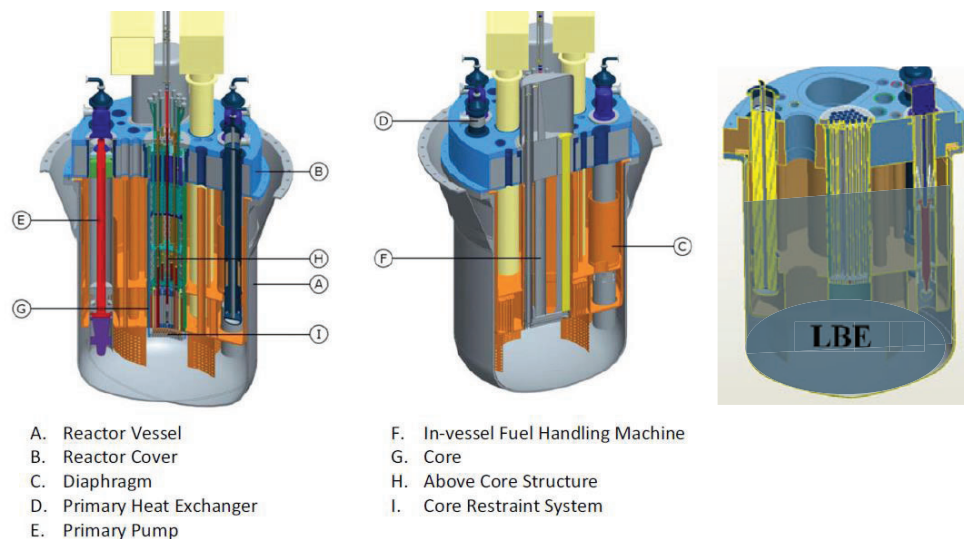

A. Reactor Vessel
B. Reactor Cover
C. Diaphragm
D. Primary Heat Exchanger
E. Primary Pump
F. In-vessel Fuel Handling Machine
G. Core
H. Above Core Structure
I. Core Restraint System

Figure 1. MYRRHA nuclear reactor schematic and level of LBE coolant.

The problem of sloshing has been studied extensively for many different applications, from aerospace and liquid transport to seismic safety of storage tanks and nuclear reactors [3,4]. Guidelines for the seismic safety of nuclear reactors were given based on simple mechanical models [1], following the work of Housner [5]. The growing capabilities of CFD codes have made numerical simulation a popular tool for the study of sloshing problems and interface capturing methods can provide accurate prediction of the sloshing behavior inside the tank [3,4,6,7]. For HLM reactors, different approaches to the problem have been proposed using Finite Element [8], Finite Volume [9] and Smooth Particle Hydrodynamics [10]. The CFD code OpenFOAM has been used to simulate sloshing in the case of HLM reactor ELSY, providing qualitative and quantitative validation for the solver [9]. In the present study, further validation of this tool is attempted by comparison with dedicated experiments.

For the experimental investigation, the possibility to use water instead of liquid metals in a laboratory environment would simplify substantially the work. However, there is not a lot of information in the literature about how LBE or other liquid metals behave in sloshing situations. To demonstrate the effect of the liquid properties on the sloshing behavior, experiments using mercury and water are presented. Mercury is used in an attempt to approximate the properties of Lead Bismuth Eutectic (LBE) for the case of MYRRHA. The geometry of the reactor is simplified to a cylindrical shape to avoid other effects on sloshing and sinusoidal excitation signals are applied. The study focuses on the resonance case, where the excitation frequency matches the first mode of the fluid in the tank, showing complex liquid motions.

2. METHODS

Sloshing is studied experimentally on a laboratory scale model with simplified geometry using mercury and water. The same test cases are simulated numerically using the CFD code OpenFOAM.

2.1. Experimental Study

Experimental investigation of the effect of the liquid properties on the sloshing behavior for the case of a cylindrical tank is carried out using optical methods. The excitation of the tank is imposed using the von Karman Institute shaking table facility named SHAKESPEARE (SHaking Apparatus for Kinetic Experiments of Sloshing Projects with EArthquake REproduction). This square shaped shaking table of 1.5 m size features 3-axis translations with three independent modules, one moving on each axis, as shown in Fig. 2. Hydraulic piston actuators are used to impose the motions of the table, controlled by a central computer through a feedback loop with position sensors. The maximum displacement is 45 mm on each axis, while the maximum acceleration is approximately 1.1 g, designed for loads up to 500 kg. The system can reproduce complex 3-axis earthquake time histories, which are loaded on the central controller, but any type of continuous signal within the aforementioned limitations can be prescribed.
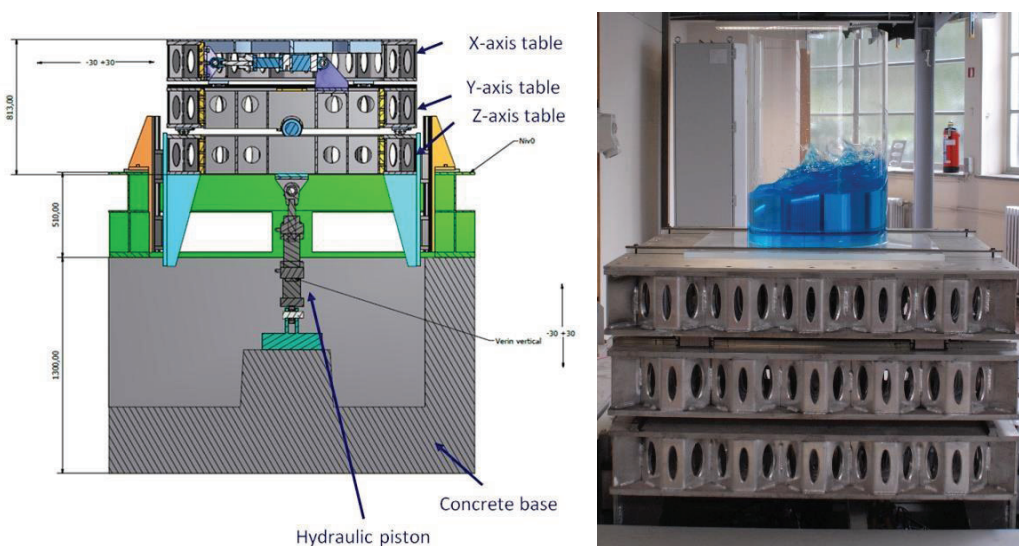

Figure 2. Shaking table facility SHAKESPEARE with schematic of three axis modules (left) and demonstration of sloshing in cylindrical tank (right).

The use of LBE in a laboratory environment poses several difficulties, as it has a melting point of 396.7 K and requires a heated tank to keep it liquid [11]. Using water for the sloshing experiments simplifies substantially the task, but verification is needed that it has similar behavior to liquid metals. For this purpose a comparison is made using water and mercury (Hg), which is liquid at room temperature and thus easier to use for sloshing. Special precautions have to be taken in the laboratory because mercury is toxic, so the tank has to be well sealed. The properties of LBE, water and mercury at their corresponding reference temperature are summarized in Table I.

Table I. Properties of different working liquids for the study of sloshing

Liquid	T_{ref} [K]	ρ [kg/m³]	ν x10⁻⁶ [m²/s]	σ [N/m]
LBE	620	10275	0.162	0.396
Water	293	998	1.004	0.073
Mercury	293	13579	0.114	0.487

The use of mercury aims at comparing the sloshing behavior of a liquid metal to the one of water at similar conditions, in order to demonstrate the effect of different liquid properties (density, viscosity, surface tension). It is noted that in general the properties of the liquid have small impact on the natural frequency, which is dominated by the size of the tank and the liquid height. Given that the sloshing effect is maximum at the case of resonance, it is very interesting to examine this case with the different liquids. Far from resonance, the liquid follows in general the excitation frequency of the tank, so it is expected that the effect on the liquid motion and the resulting forces will be smaller.

A problem that is often addressed in experimental studies of sloshing is the *scaling* of the model. As in most applications the laboratory model is made at a reduced scale, similarity of the problem has to be respected. Scaling rules can be obtained from dimensional analysis [12]. For the case of a cylindrical tank with radius R, filled up to height h with liquid and subjected to sinusoidal excitation $X = A \sin(\omega t)$, with g the gravitational acceleration, ρ the liquid density, v the kinematic viscosity and σ the surface tension, with the subscripts m and p indicating model and prototype respectively, some main aspects of similarity that should be respected when simulating sloshing are:

- **Geometric similarity**: h/R. The geometric similarity indicates that the ratio of liquid height (fill level) to tank size should be respected: $h_m/h_p = R_m/R_p$.
- **Froude number**: $Fr = U^2/gR$. The kinematic similarity where the velocity $U \sim A\omega$ results in the ratio of excitation amplitude to length scale A/R to be respected, suggesting $A_m/A_p = R_m/R_p$. It is also implied that the natural frequency $\omega_n^2 \sim g/R$ will be used to keep the ratio ω^2/ω_n^2.
- **Reynolds number**: $Re = UL/v$ and by substituting the characteristic velocity U becomes $Re = A\omega R/v$. The dynamic similarity results in the ratio $\omega_m/\omega_p = (v_m/v_p)(A_p/A_m)(R_p/R_m)$, which is very difficult to respect, as the properties of the liquid become a limiting factor for the frequencies. When the viscosity effects are not dominant, the Re similarity can be relaxed.
- **Euler number**: $Eu = F/\rho$ a L^3, with F the force and L the length scale. The ratio of forces is expressed as $F_m/F_p = (\rho_m/\rho_p)(a_m/a_p)(R_m/R_p)^3$.
- **Bond number**: $Bo = \rho g L^2/\sigma$. It relates the gravitational with the surface tension effects and when gravity is present usually $Bo >> 1$, indicating that surface tension effects are negligible.

The scaling parameters suggest that for different liquids in the same tank with identical acceleration, the forces should scale with the ratio of densities. Viscous effects and surface tension are expected to have much smaller contribution.

To investigate experimentally the effect of liquid properties, a small scale cylindrical tank is used to model the reactor. The radius of the tank is $R = 0.06$ m, and the liquid height h=0.135 m, keeping the same ratio as in MYRRHA ($h/R = 2.25$) with a scale of 1/66. The total height of the tank is higher than in the case of the real reactor, leaving about 0.1 m from the liquid surface to the cover of the tank to allow for free movement of the surface without hitting the cover. Two cylindrical tanks with the same dimensions are made from Plexiglas, with the one for mercury featuring a supporting base from steel to hold the increased weight.

The natural frequencies of the tank are calculated using the expression:

$$\omega_{m,n}^2 = \frac{g\xi_{m,n}}{R} \tanh\left(\frac{\xi_{m,n}h}{R}\right) \tag{1}$$

where for antisymmetric modes $m = 1 : \xi_1 = 1.841, \xi_2 = 5.335, ... \xi_n \rightarrow \xi_{n-1} + \pi$ [3]. The first and second sloshing modes are computed for the tank first without taking into account the liquid properties, resulting in a first mode at 2.77 Hz and second mode at 4.7 Hz. When surface tension is taking into account, the natural frequency will be slightly higher for mercury, but the difference is negligible for this case. Three different frequencies are tested, one lower than the first sloshing mode at 1.5 Hz, one at the natural

frequency of 2.77 Hz and one higher at 3.5 Hz. Different amplitudes of excitation of 1.5, 2.5, 5 and 10 mm are applied.

The sloshing behavior in the tank is followed using high speed visualization. Videos are recorded with a Phantom v.7 high-speed camera, mounted on the sloshing table with the container illuminated from the back, resulting in a form of visualization resembling shadowgraphy. Between the container and the lamp a plate of opaque glass is used to create diffuse lighting. The setup is presented in Fig. 3. Due to the opaque nature of mercury, no light is allowed to pass from it. On the other hand water is transparent, but the interface casts a shadow over the image, resulting in high contrast for the interface detection.
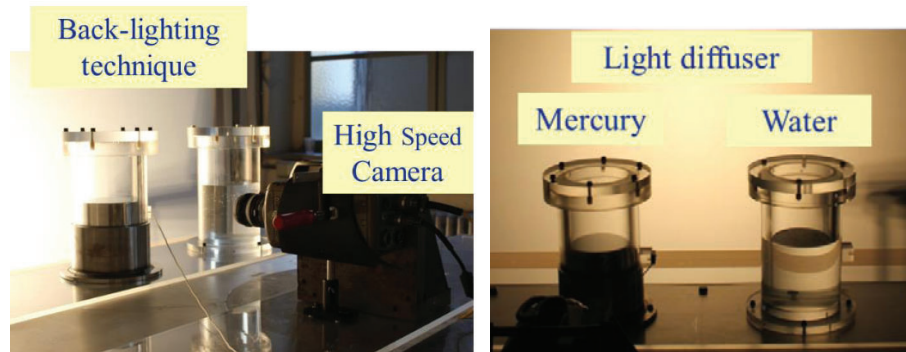

Figure 3. Back-lighting technique for experimental study of sloshing using mercury and water.

Applying digital image processing, the liquid elevation is tracked by identifying the interface at the top of the darker area in the image, as shown in Fig. 4 for mercury and water. When large waves and high surface deformation occur, it is more difficult to locate the interface, which results in high uncertainty for the method. Moreover, other difficulty is the presence of droplets on the cylindrical surface of the tank, but it is possible to remove those points by applying a mask on the image.
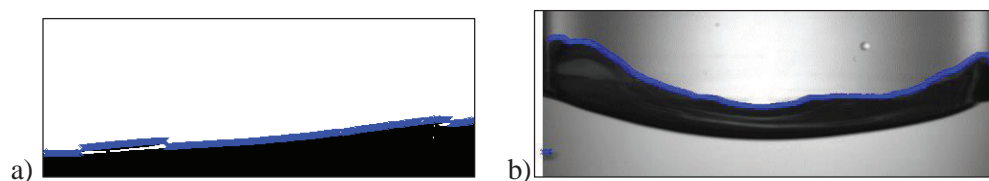

Figure 4. Interface position from digital image processing for a) mercury and b) water.

2.2. Numerical Approach

To study the sloshing phenomena inside the partially filled tank, a CFD approach is taken using the open source code OpenFOAM. To model this multiphase problem the Volume of Fluid (VOF) method is applied, allowing to track the position of the liquid-gas interface. The governing equations for two isothermal, incompressible, immiscible fluids include the continuity and momentum equations:

$$\nabla \cdot \mathbf{V} = 0 \qquad (2)$$

$$\frac{\partial(\rho\mathbf{V})}{\partial t}+\nabla\cdot(\rho\mathbf{V}\mathbf{V})=-\nabla p+\nabla\cdot\tau+\rho\mathbf{g}+\mathbf{F}_\sigma \tag{3}$$

where ρ is the fluid density, $\mathbf{V}$ the fluid velocity vector, τ the viscous stress tensor defined as $\tau = 2\mu(1/2[[(\nabla V)]+(\nabla V)^T])$, p the scalar pressure, $\mathbf{F}_\sigma$ the volumetric surface tension force and $\mathbf{g}$ the gravitational acceleration.

The VOF method was first developed by Hirt and Nichols [13] and tracks the interface using the volume fraction function a, where $0 \le a \le 1$. The cells with $a = 1$ are filled with the liquid phase, $a = 0$ indicates the gas phase, and the cells where $0 < a < 1$ contain the interface. The interface advection equation is expressed as:

$$\frac{\partial a}{\partial t}+\nabla\cdot(a\mathbf{V})=0 \tag{4}$$

The fluid domain is defined for a single mixture where the function a is used to distinguish between the two fluids. The physical properties of the two immiscible fluids are calculated using a weighted average:

$$\rho = a\rho_l + (1-a)\rho_g, \quad \mu = a\mu_l + (1-a)\mu_g \tag{5}$$

where the subscripts l and g stand for the liquid and the gas, respectively.

For large density ratios, the main challenge for advecting the a function is to preserve the mass conservativeness while guaranteeing boundedness. OpenFOAM uses an algebraic approach based on the counter-gradient transport to advect the volume fraction a. This scheme adds a compressive term to the a advection equation in order to retain the conservativeness, convergence and boundedness [14]. The advection equation is re-formulated as:

$$\frac{\partial a}{\partial t}+\nabla\cdot(\mathbf{V}a)+\nabla\cdot(\mathbf{V}_c a(1-a))=0 \tag{6}$$

where $\mathbf{V}_c = \mathbf{V}_l - \mathbf{V}_g$ is the compressive velocity [15]. The compressive velocity is taken into consideration only in the region of the gas-liquid interface and it is calculated in the normal direction to the interface to avoid any dispersion. Moreover, a compressive factor c_a is used to increase compression as:

$$\mathbf{V}_c = \min\left(c_a|\mathbf{V}|, \max(|\mathbf{V}|)\right)\frac{\nabla a}{|\nabla a|} \tag{7}$$

The volume fraction advection equation is solved using the MULES method which is based on the method of flux corrected transport where an additional limiter is used to cutoff the face-fluxes at the critical values [16]. OpenFOAM solves the above equations based on the Finite Volume method, employing a segregated solver approach (PISO algorithm) for pressure-velocity calculations. For the simulations presented here, no turbulence model was used and a neutral contact angle of 90° was set for both mercury and water. An unstructured mesh of about 700,000 quad cells is used, with typical cell size of 1.6 mm and typical time step of 10^{-4} s.

To apply an excitation to the tank and induce sloshing, a dynamic mesh algorithm is coupled with the VOF method, introducing a solid body motion of the entire domain of the vessel in six degrees of freedom [17]. In this way it is possible to prescribe any kind of continuous excitation time history, where a tabulated description of the motion in time is provided and interpolation is applied to compute the position of the mesh in each time step.

3. RESULTS

A comparison of the sloshing behavior for mercury and water is carried out applying sinusoidal lateral excitation to the cylindrical tank. The sloshing response depends highly on the frequency of the excitation and the maximum effect is observed when the forcing frequency matches the natural frequency of the tank, a case known as *resonance*. This corresponds to the first antisymmetric mode of the system, which leads to large wave amplitude and displacement of the center of gravity for the liquid inside the tank. Resonance is a worst case scenario for the safety analysis, as the forces exerted on the tank take the maximum values. Most sloshing studies examine the two first antisymmetric modes of the tank, as from the third mode onwards the effects from sloshing are rather small [3,12].

From the experimental study it is observed that if the amplitude of the excitation is small compared to the tank radius and the excitation frequency is lower than the natural frequency, then the liquid elevation in the tank is also small. In this regime of *linear* sloshing the liquid elevation increases for larger excitation amplitudes, while the interface shape remains similar (half cosine wave with small amplitude in 2D). The sloshing behavior in this case does not change for different working liquids, as it shown for the comparison between mercury and water in Fig. 5, where the amplitude of the sinusoidal excitation is X_o=0.0025 m and the frequency f =1.5 Hz (Ω = 9.425 rad/s).
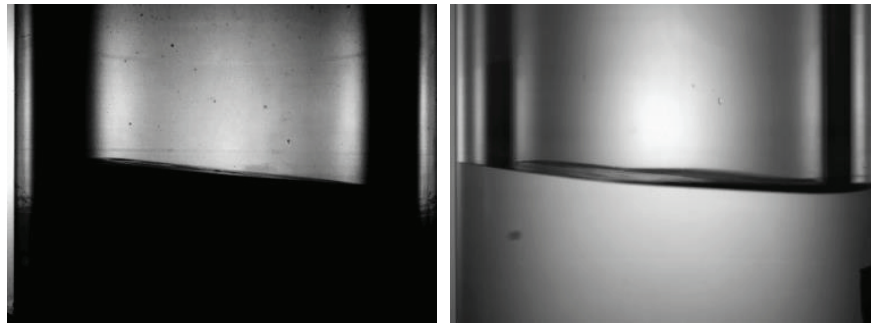

Figure 5. Maximum liquid elevation for linear sloshing case with sinusoidal excitation X=X$_o$sin(Ωt), X$_o$=0.0025 m, Ω=9.425 rad/s for mercury (left) and water (right).

The *resonance* case is interesting for the safety study and is investigated further with the two working liquids. In the presented case the excitation frequency matches the natural frequency for the cylindrical tank, which is 2.77 Hz, with an amplitude of 0.0025 m. The sloshing behavior in resonance is non-linear, while the liquid elevation and the forces on the walls theoretically tend to infinity. In practice the damping effect due to viscosity limits the liquid elevation, but eventually the liquid rises so high in the tank that breaking waves appear. Another particular phenomenon that appears in symmetric tanks is that the liquid can start rotating around the tank, which is known as *swirling* [3,4]. Such behavior occurs when some liquid moves off the axis of the forcing and starts to excite the natural modes in the other horizontal direction. The result is rather spectacular, with a large part of the liquid rising high on the tank walls and

being accelerated in a sweeping motion around the tank wall (Fig. 6). This can be very dangerous for the structure, as it applies a large horizontal force repeatedly on the cylindrical part.
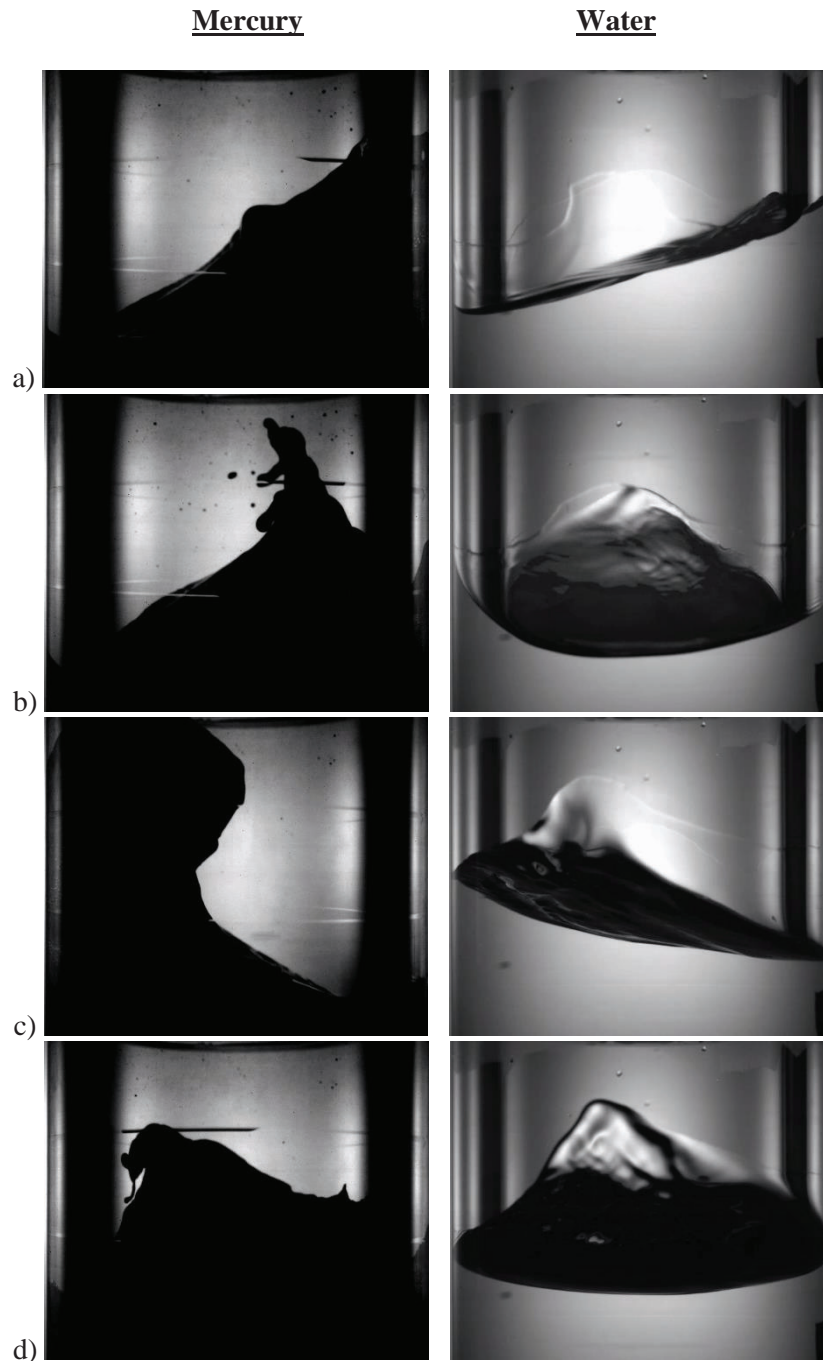
Mercury   **Water**

Figure 6. Visualization of sloshing in cylindrical tank (R=0.06 m) for resonance case (sinusoidal forcing X_0= 0.0025 m, Ω = 17.4 rad/s) with mercury (left) and water (right). Instantaneous results with a) large liquid elevation and non-linear sloshing, b) breaking waves and ejection of ligaments and droplets for mercury, c,d) swirling and large waves on the tank walls.
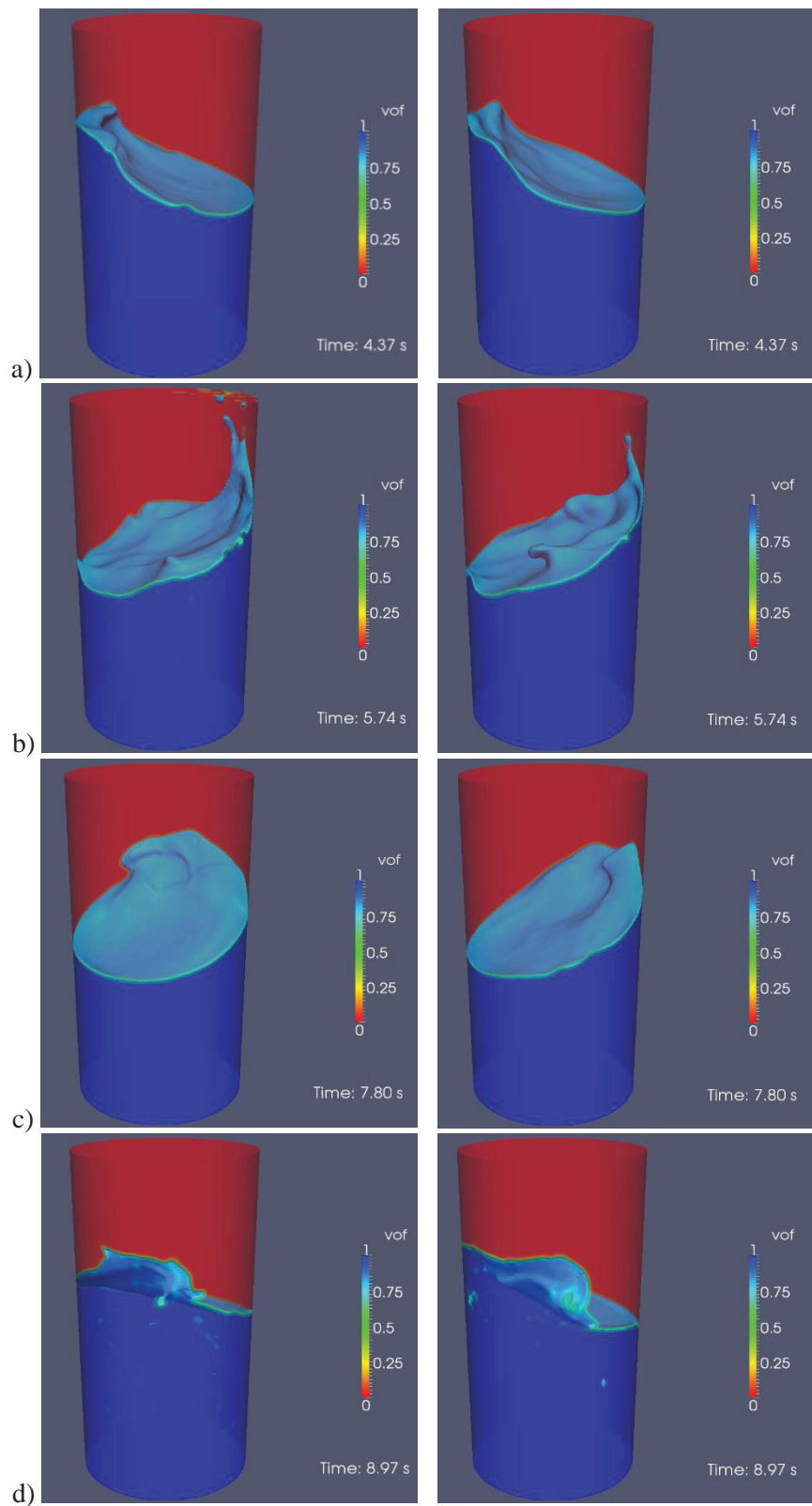
Mercury   **Water**

Figure 7. Simulation of sloshing in resonance case with a=0.0025m and Ω = 17.4 rad/s with mercury (left) and water (right). Instantaneous results at a) 4.37s with non-linear sloshing, b) 5.74s when droplets are ejected, c) 7.80s when swirl begins, d) 8.97s with breaking waves.

A comparison of the behavior of mercury and water in resonance is presented in Fig. 6. The visualization shown is taken after the first transient cycles, where the liquid enters the swirl. For mercury larger sloshing waves appear as a result of higher density and lower viscosity. At the limit of one-axis sloshing, ligaments and droplets are ejected from the liquid body, reaching the cover of the tank (0.1 m above the undisturbed surface). The higher surface tension of the liquid metal helps these formations. The rotating motion accelerates and decelerates periodically, with mercury covering almost all the height of the tank. This results in a dark image, so the image processing is very difficult for this case. On the other hand water appears more stable, with higher damping and lower liquid elevation in the tank. While in rotation the liquid still reaches large heights on the tank wall, overall the behavior is more periodic with limited range.

The same case is simulated numerically using OpenFOAM, as described in Section 2.2, for a total of 36 s of physical time. A series of instantaneous results from the simulation using mercury and water is presented in Fig. 7. In the beginning the liquid is rising from side to side as the excitation is only on the X-axis, with increasing height (a), until it splashes to the top of the tank (b). Then the sloshing reduces until it passes to a rotating motion (c) which continues until the end of the simulation. The liquid in rotation is periodically accelerated and occasionally breaking waves form on the wall (d) where the interface folds on itself. The numerical simulations are able to capture well the complex sloshing behavior that takes place in the tank, with non-linear sloshing, splashing and swirling. Mercury and water are shown to behave similarly, with only small differences mainly in the interface shape.

The maximum liquid elevation recorded in time for the cases with mercury and water is presented in Fig. 8 for a) the numerical results and b) the experiments. The numerical results are obtained by tracking the position of the interface (volume fraction 0.5) in all the cylindrical domain and taking the maximum height. It is shown that the maximum liquid elevation increases for the first forcing cycles, until the response becomes non-linear. For mercury droplets are ejected and eventually they reach the top of the tank (0.1 m), while for water the height is lower. When rotation starts (from 7 s), mercury rises faster on the tank wall and reaches a little larger elevation than water. Then the swirl becomes more periodic, with cycles of increasing and decreasing amplitude, characterized by a low frequency.

The experimental results for the maximum liquid elevation are obtained from digital image processing and are shown in Fig. 8.b. The recording did not start from the beginning of the sloshing motion, but when the swirl was already established. The signal for mercury shows that in the initial phase of recording, the liquid has reached the top of the tank. Since mercury is opaque, the image is dark and no detailed analysis is possible. Later the liquid height decreases and the maximum value varies from 40 to 70 mm. Then another cycle of splashing and large waves occurs for mercury. For water, the signal is more stable and the maximum value is between 25 and 55 mm, which is lower than for mercury. It is found that the liquid elevation changes not only during a period, but also at lower frequencies, representing the repeated cycles of swirling.

The comparison between numerical and experimental results for mercury can be made after the liquid has reached the top of the tank (about 6 s) and the maximum elevation is reduced, indicating that swirling has started. The values of maximum elevation and the time evolution is in good agreement for simulations and experiments. The low frequency in the swirling cycles (increasing-decreasing elevation) is also well captured numerically. However, the repeated splashing and tall waves are not observed in the simulations, after the initial occurrence. Mercury and water appear to behave more similarly than what is observed experimentally. For water, the maximum elevation values are also close, but slightly higher variation is

predicted numerically. In the experiments the rotating motion is very stable, with small changes in amplitude. In the quantitative comparison, it has to be noted that in the experiments a projection of the liquid surface over the image plane is taken, while in simulations the value represents the 3D domain. As the surface oscillates and deforms, higher uncertainty is introduced in the measurements. For water especially, the internal wall of the tank can remain wetted during the swirling, showing higher elevation than in reality. Overall the sloshing behavior is satisfactorily predicted, taking into account the complexity of the physical phenomena. The occurrence of splashing to the top of the tank, the transition to the swirling motion and the low frequency cycles are all captured from the CFD tool. Points to be improved in the numerical simulations include the evaluation of turbulence modeling, especially in the resonance case where strong liquid motions are observed. Moreover, more realistic modeling of the contact angle can be introduced, as for water it is expected to be about 80° and for mercury close to 140°.
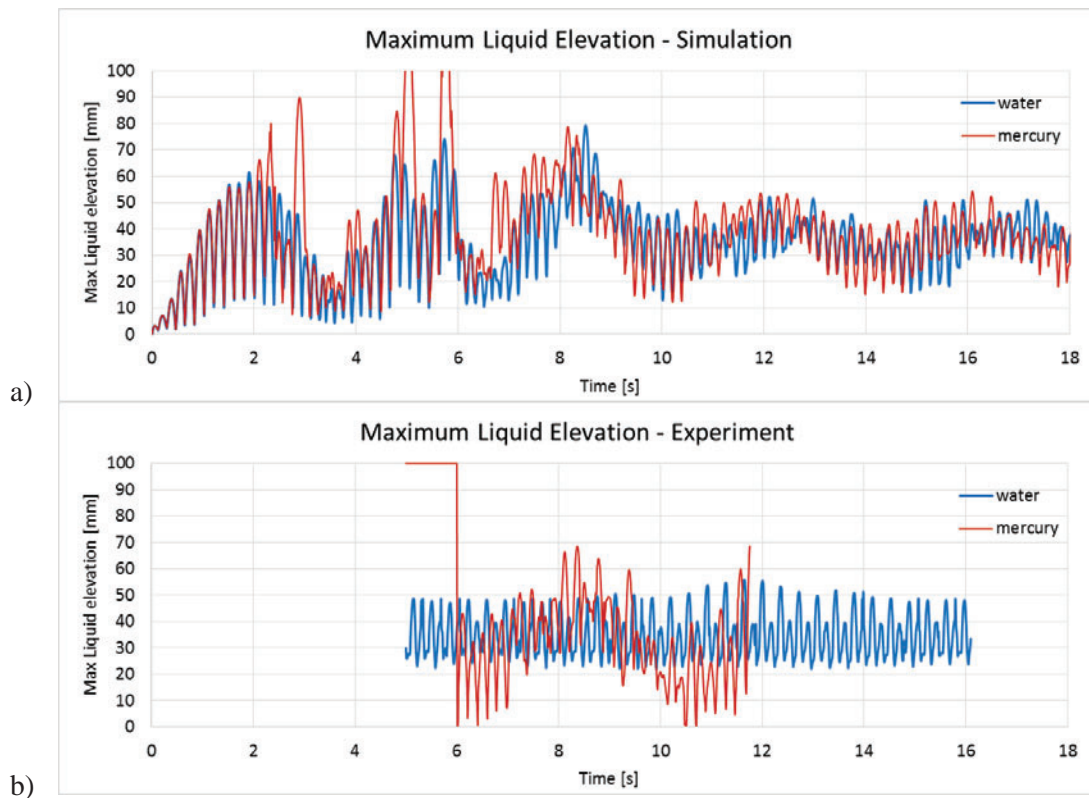
a)

b)

Figure 8. Maximum liquid elevation in time for the case of mercury and water from a) numerical simulations and b) experiments.

The forces that are exerted on the tank are extracted from the numerical results by integrating the pressure on the tank walls. The results for mercury and water are presented in Fig. 9, with a) the signal in X direction, b) in Y direction and c) in the vertical Z direction. For the case of mercury the forces are normalized by the density ratio $\rho_{Hg}/\rho_{H2O} = 13.6$, allowing the comparison of the sloshing behavior of the two liquids.

From the forces in X-direction in Fig. 9.a, it is observed that in the first 7 seconds both liquids exhibit a motion on X-axis, while after they enter a rotating motion where the force increases considerably. The Y component of the force in Fig. 9.b is shown to grow after 5s and when the rotation starts it follows an

evolution similar to the X component. The amplitude of the forces scales well with the density ratio, which shows that the effect of sloshing is similar for the two liquids. The frequency matches the forcing frequency in both cases. For the Z-component of the force in Fig. 9.c variations around the value of the total liquid weight are presented. The variations in this direction are higher initially but lower for the rotating regime. The frequency of the signal is double the forcing frequency, as the minimum force occurs twice in a period. In general, it is seen that while the amplitude of normalized forces and frequencies are similar for the two liquids, there is a phase difference, indicating that mercury starts rotating and stops faster than water. This can be attributed to reduced damping due to lower viscosity.
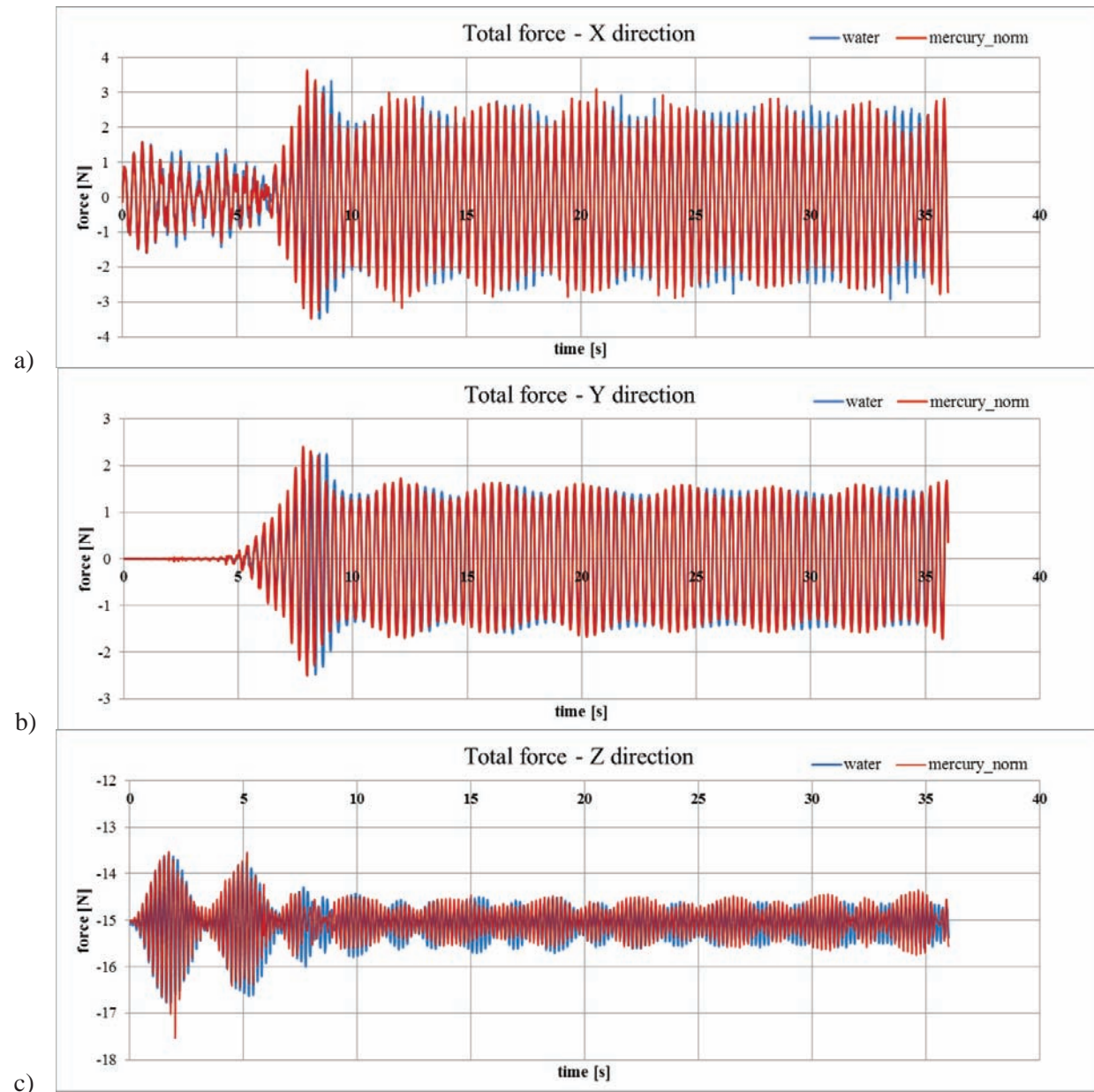

Figure 9. Total forces on the tank during the simulation for water and normalized forces for mercury for a) X-axis, b) Y-axis and c) Z-axis (vertical).

The numerical results show that the estimated forces follow a similar evolution in time and their amplitude scales with the density ratio of the liquids, as expected from dimensional analysis. Comparison against experimental results remains to be performed to complete the validation. The comparison between mercury and water is made for the resonance case, where the maximum difference is observed for the shape of the liquid surface and the maximum elevation, while for linear sloshing the differences are much smaller. In these cases, when water is used in a laboratory scale model, the force in the case of the MYRRHA reactor with liquid metal can be calculated by applying the suggested scaling rules.

4. CONCLUSIONS

Sloshing in a HLM reactor under seismic excitation can induce additional forces on the structures, requiring good prediction tools. A study on a simplified cylindrical model applying sinusoidal excitation is carried out using CFD and the results are compared with dedicated experiments for validation. The application of similarity rules for the scaling of the experimental model is discussed. The effect of the properties of liquid metal on the sloshing behavior is demonstrated experimentally comparing mercury and water.

Generally the two liquids behave similarly, with the maximum difference in the interface shape occurring at resonance. In this case non-linear sloshing and swirling are observed. The maximum liquid elevation shows differences between mercury and water, with higher values for mercury, where ejection of droplets and ligaments from the liquid are observed.

The complex behavior of the resonance case is captured well by the numerical simulations, including non-linear sloshing with ejection of droplets, breaking waves, transition to swirling and low frequency variations of the liquid elevation in the tank. Quantitative comparison of the maximum liquid elevation shows good agreement with experiments on the range of variation. Some discrepancies are observed on the dynamic behavior of the liquids, which are predicted to be more similar than the experimental observation. The forces on the tank walls are also extracted from CFD, verifying that their amplitude scales with the density ratio, while the time evolution is rather similar for mercury and water. Comparison with measured forces in experiments remains as a next step for the validation.

It is concluded that using water to evaluate the forces and sloshing effects on the reactor model is a valid option for frequencies up to the first sloshing mode, but should be used with caution for resonance and higher frequencies. Moreover, the CFD simulations with the VOF method show good capabilities for the prediction of sloshing phenomena in HLM nuclear reactors.

ACKNOWLEDGMENTS

REFERENCES

1. T.H. Thomas et al., "Nuclear reactors and earthquakes," *US Atomic Energy Commission, TID-7024*, Chapter 6, pp. 183-209 (1963).

2. P. Baeten, M. Schyns, R. Fernandez, D. De Bruyn, and G. Van den Eynde, "MYRRHA: A multipurpose nuclear research facility," *EPJ Web of Conferences*, vol. 79, p. 03001, EDP Sciences (2014).

3. R.A. Ibrahim, *Liquid sloshing dynamics: theory and applications*, Chapters 1-3, Cambridge University Press, Cambridge, UK (2005).

4. O.M. Faltinsen and A.N. Timokha, *Sloshing*, Chapters 1, 2, 4, 10, Cambridge University Press, Cambridge, UK (2009).

5. G. W. Housner, "Dynamic pressures on accelerated fluid containers," *Bulletin of the Seismological Society of America*. **47**(1), pp. 15–35 (1957).

6. J. Mahaffy, B. Chung, C. Song, F. Dubois, E. Graffard, F. Ducros, M. Heitsch et al., *Best practice guidelines for the use of CFD in nuclear reactor safety applications*, Organisation for Economic Co-Operation and Development, Nuclear Energy Agency-OECD/NEA, Committee on the safety of nuclear installations-CSNI, OECD Publishing, Paris, France (2007).

7. F. Roelofs, V. R. Gopala, K. Van Tichelen, X. Cheng, E. Merzari and W. D. Pointer, "Status and future challenges of CFD for liquid metal cooled reactors," In *IAEA FR13* (2013).

8. D. Aquaro and G. Forasassi. "Sloshing effects of ADS-DF lead-bismuth primary coolant caused by the reference earthquake," *Proceedings of 18th international conference on structural mechanics in reactor technology (SMiRT 18)*, Beijing, China, August 7-12, pp. 315-326 (2005).

9. V.R. Gopala and F. Roelofs, "Numerical simulation of liquid lead sloshing in the ELSY reactor vessel," *Fifth International Workshop on Materials for HLM-cooled Reactors and Related Technologies (HeLiMeRT)*, Mol, Belgium, April 20-22, 2009, pp. 135-147 (2009).

10. A. Vorobyev, V. Kriventsev and W. Maschek, "Simulation of central sloshing experiments with smoothed particle hydrodynamics (SPH) method," *Nucl. Eng. Des.* **241**(8), pp. 3086-3096 (2011).

11. G. Benamati and V. Sobolev, *Handbook on lead–bismuth eutectic alloy and lead properties, materials compatibility, thermal-hydraulics and technologies*, Chapter 2: Thermophysical and electric properties, Organisation for Economic Co-Operation and Development, Nuclear Energy Agency-OECD/NEA, Working Party on Scientific Issues of the Fuel Cycle, Working Group on Lead-bismuth Eutectic, OECD Publishing, Paris, France, pp. 25-99 (2007).

12. H.N. Abramson, *The dynamic behavior of liquids in moving containers, with applications to space vehicle technology*, Chapter 5, NASA SP-106, Washington, USA (1966).

13. C.W. Hirt and B.D. Nichols, "Volume of fluid (VOF) method for the dynamics of free boundaries," *J. Comp. Phys.* **39**(1), pp. 201-225 (1981).

14. H.G. Weller, "A new approach to VOF-based interface capturing methods for incompressible and compressible flow," *OpenCFD Ltd., Report TR/HGW/04* (2008).

15. E. Berberović, N.P. van Hinsberg, S. Jakirlić, I.V. Roisman and C. Tropea, "Drop impact onto a liquid layer of finite thickness: dynamics of the cavity evolution," *Physical Review E* **79,** pp. 036306 (2009).

16. S.T. Zalesak, "Fully multidimensional flux-corrected transport algorithms for fluids," J. Comput. Phys. **31**, pp. 335–362 (1979).

17. H. Jasak and Z. Tukovic, "Dynamic mesh handling in openfoam applied to fluid-structure interaction simulations," *Proceedings of the V European Conference Computational Fluid Dynamics,* Lisbon, Portugal, June 14-17, (2010).